Title

Progerin forms an abnormal meshwork and has a dominant-negative effect on the nuclear lamina

Journal

Proceedings of the National Academy of Sciences of the United States of America, 121(27)

ISSN

0027-8424

Authors

Kim, Paul H
Kim, Joonyoung R
Tu, Yiping
et al.

Publication Date

2024-07-02

DOI

10.1073/pnas.2406946121

Peer reviewed

PNAS RESEARCH ARTICLE | MEDICAL SCIENCES

Progerin forms an abnormal meshwork and has a dominant-negative effect on the nuclear lamina

Paul H. Kim[a,b], Joonyoung R. Kim[a], Yiping Tu[a], Hyesoo Jung[a], J. Y. Brian Jeong[c], Anh P. Tran[a], Ashley Presnell[a], Stephen G. Young[a,d,1], and Loren G. Fong[a,1]

Affiliations are included on p. 11.

Contributed by Stephen G. Young; received April 15, 2024; accepted May 28, 2024; reviewed by Susan Michaelis and Howard J. Worman

Progerin, the protein that causes Hutchinson–Gilford progeria syndrome, triggers nuclear membrane (NM) ruptures and blebs, but the mechanisms are unclear. We suspected that the expression of progerin changes the overall structure of the nuclear lamina. High-resolution microscopy of smooth muscle cells (SMCs) revealed that lamin A and lamin B1 form independent meshworks with uniformly spaced openings (~0.085 μm^2). The expression of progerin in SMCs resulted in the formation of an irregular meshwork with clusters of large openings (up to 1.4 μm^2). The expression of progerin acted in a dominant-negative fashion to disrupt the morphology of the endogenous lamin B1 meshwork, triggering irregularities and large openings that closely resembled the irregularities and openings in the progerin meshwork. These abnormal meshworks were strongly associated with NM ruptures and blebs. Of note, the progerin meshwork was markedly abnormal in nuclear blebs that were deficient in lamin B1 (~50% of all blebs). That observation suggested that higher levels of lamin B1 expression might normalize the progerin meshwork and prevent NM ruptures and blebs. Indeed, increased lamin B1 expression reversed the morphological abnormalities in the progerin meshwork and markedly reduced the frequency of NM ruptures and blebs. Thus, progerin expression disrupts the overall structure of the nuclear lamina, but that effect—along with NM ruptures and blebs—can be abrogated by increased lamin B1 expression.

progeria | smooth muscle cells | nuclear membrane ruptures | nuclear lamina | high-resolution confocal microscopy

Significance

Progerin, the mutant lamin A in the pediatric progeriod disorder Hutchinson–Gilford progeria syndrome, triggers disease despite persistent synthesis of wild-type lamin A, prompting speculation that progerin acts in a dominant-negative fashion to disrupt the structure and function of the nuclear lamina. Thus far, however, there have been no quantitative studies linking structural changes to the nuclear lamina with progerin-induced effects in cells. We showed that progerin forms an abnormal meshwork with large openings and that it triggers remarkably similar abnormalities in the meshwork formed by lamin B1 (i.e., arguably a dominant-negative effect). These structural abnormalities, along with nuclear membrane ruptures and nuclear blebs, could be reversed by increased expression of lamin B1 or the inner nuclear lamin membrane protein LAP2β.

Hutchinson–Gilford progeria syndrome (HGPS), a progeroid disorder in children, is caused by the synthesis of progerin, a mutant form of prelamin A (1). Children with HGPS develop disease phenotypes in multiple tissues (e.g., bone, connective tissue, skin, hair, heart, vasculature) and typically die during their teenage years from atherosclerotic cardiovascular disease (2). Progerin is caused by a de novo point mutation in *LMNA* [most often p.G608G(GGC>GGT)] that promotes the usage of a cryptic splice donor site and leads to a mutant transcript with an in-frame deletion of 150 nucleotides, resulting in the production of progerin, an internally truncated prelamin A that retains a C-terminal farnesyl lipid anchor (3). Progerin is unequivocally the culprit in HGPS. The expression of progerin in genetically modified mice triggers disease phenotypes similar to those in children with HGPS (e.g., skeletal abnormalities, osteoporosis, alopecia, vascular disease, sclerodermatous changes in the skin) (4–6). When progerin is expressed in cultured cells, it triggers phenotypes that are observed in fibroblasts from children with HGPS (e.g., abnormal nuclear shape, DNA damage, senescence) (1, 7).

Progerin is targeted to the nuclear lamina, an ~14 nm-thick fibrillar structure (in mouse embryonic fibroblasts) located adjacent to the inner nuclear membrane (NM) (8). In most somatic cells, the main components of the nuclear lamina are the A-type lamins (lamin A and lamin C; products of *LMNA*) and the B-type lamins (lamin B1 and lamin B2; products of *LMNB1* and *LMNB2*, respectively) (9). The A- and B-type lamins assemble into separate but interacting net-like fibrillar meshworks (10–12). The nuclear lamina provides structural support for the nucleus and protects the integrity of the NMs. Fibroblasts lacking all nuclear lamins (*Lmna*$^{-/-}$*Lmnb1*$^{-/-}$*Lmnb2*$^{-/-}$) exhibit frequent and prolonged NM ruptures, resulting in DNA damage (13). Nuclear lamins also interact with NM proteins, DNA-binding proteins, and transcription factors impacting critical cellular functions (e.g., cell migration, heterochromatin anchoring, nuclear positioning, gene expression, cell division) (14).

When progerin is expressed in cultured cells, it alters properties associated with the nuclear envelope (7, 15–20). In smooth muscle cells (SMCs), progerin increases nuclear stiffness, as judged by atomic force microscopy (21). It also triggers replicative stress (22),

Author contributions: P.H.K. and L.G.F. designed research; P.H.K., J.R.K., Y.T., H.J., J.Y.B.J., A.P.T., A.P., and L.G.F. performed research; P.H.K., J.R.K., Y.T., A.P.T., A.P., and L.G.F. contributed new reagents/analytic tools; P.H.K., J.R.K., Y.T., S.G.Y., and L.G.F. analyzed data; and P.H.K., S.G.Y., and L.G.F. wrote the paper.

Reviewers: S.M., Johns Hopkins University School of Medicine; and H.J.W., Columbia University.

The authors declare no competing interest.

[1]To whom correspondence may be addressed. Email: sgyoung@mednet.ucla.edu or lfong@mednet.ucla.edu.

This article contains supporting information online at https://www.pnas.org/lookup/suppl/doi:10.1073/pnas.2406946121/-/DCSupplemental.

Published June 25, 2024.

reduced DNA repair (23), ER stress (24), DNA damage and NM ruptures (21). Progerin also renders nuclei of SMCs more susceptible to mechanical stress, resulting in increased numbers of NM ruptures, greater DNA damage, and more cell death (21, 25). In a mouse model of HGPS, we observed NM ruptures in SMCs in the medial layer of the aorta (21). The fact that progerin triggered NM ruptures in SMCs (but not in adjacent endothelial cells or adventitial cells) helped to explain the histopathologic hallmark in HGPS (loss of medial SMCs in large arteries) (26).

While the expression of progerin promotes nuclear blebs and NM ruptures, the mechanisms have not been clear. We formulated a simple hypothesis—that progerin expression results in overt structural abnormalities in the nuclear lamina—not only in the progerin meshwork but also in the meshworks of other nuclear lamins. To test this hypothesis, we used doxycycline (Dox)-inducible vectors to create SMCs that express prelamin A (which is processed to mature lamin A) as well as SMCs that express progerin. With these inducible cell lines in hand, we were able to characterize cells that produced identical amounts of progerin or mature lamin A. We were also able to compare, by high-resolution confocal fluorescence microscopy (11, 12), the structure of the nuclear lamina meshwork formed by progerin, and the meshwork formed by mature lamin A. These studies allowed us to test whether the structure of the progerin meshwork was abnormal, and if so, whether progerin adversely affected the structure of meshworks of other nuclear lamins (e.g., lamin B1). We were also able to determine whether abnormalities in nuclear lamin meshworks were associated with NM ruptures and blebs. We also used live cell imaging to investigate the relationship between NM ruptures and blebs.

With our studies underway, it was quickly evident that the lamin A meshwork in SMCs was uniform and regular, whereas the progerin meshwork was irregular and contained large gaps. We also found that an abnormal progerin meshwork was associated with low levels of lamin B1. The latter observation prompted us to test whether increased lamin B1 expression would eliminate the structural irregularities in the progerin meshwork, and if so, whether that would be accompanied by reduced numbers of NM ruptures and blebs.

Results

The Nuclear Lamin Meshwork Is Abnormal in Progerin-Expressing SMCs. Nuclear lamins assemble into filamentous meshworks adjacent to the inner NM. To characterize progerin and lamin A meshworks, we used Dox-inducible vectors to create clonal aortic SMCs that expressed human progerin or human prelamin A (which is processed to mature lamin A). Dox levels in the medium were adjusted to achieve progerin and lamin A levels similar to levels in the aorta of *Lmna*$^{G609G/+}$ mice (Fig. 1*A*). After 48 h of Dox induction, SMCs were stained with an antibody that detects human lamin A and progerin (but not mouse lamin A/C). The short exposure time with progerin is insufficient to affect lamin B1 levels (Fig. 1*A*). Images of the nuclear lamin meshwork at the upper surface of the nucleus (above the middle of the nucleus) were collected by high-resolution confocal fluorescence microscopy (Fig. 1*B*). Human lamin A formed a meshwork with uniform gaps of ~0.085 μm^2. The meshwork in ~80% of progerin-expressing SMCs appeared indistinguishable from lamin A–expressing cells; however, ~20% of the progerin-expressing cells exhibited an abnormal meshwork with irregularities and large gaps (Fig. 1 *B* and *C*). These observations were confirmed by super-resolution STED microscopy (Fig. 1*D*). The gaps in the abnormal regions of the progerin meshwork ranged in size from 0.01 to 1.4 μm^2 (vs. 0.01 to 0.27 μm^2 in the lamin A meshwork) and on average were larger (0.25 vs. 0.085 μm^2 in prelamin A–expressing SMCs) (Fig. 1 *E* and *F*). Both human lamin A and human progerin could form meshworks containing endogenous mouse lamin A.

Progerin Has a Dominant-Negative Effect on the Structure of the Meshworks Formed by Other Nuclear Lamins. We examined the lamin B1 meshwork in SMC lines that expressed progerin, prelamin A, or a nonfarnesyl-progerin in which the *CaaX* motif was changed from –CSIM to –SSIM (15) (*SI Appendix*, Fig. S1*A*). The endogenous lamin B1 meshwork in wild-type SMCs and prelamin A–expressing SMCs was regular, with openings averaging ~0.08 μm^2 (Fig. 2 *A* and *B*). Progerin expression changed the structure of the lamin B1 meshwork (Fig. 2 *A* and *B*), resulting in irregularities and large openings that mirrored the abnormalities in the progerin meshwork, as judged by confocal (Fig. 2*A*) and STED (Fig. 2*C*) microscopy. The gaps in the lamin B1 meshwork in progerin-expressing SMCs were larger than in prelamin A–expressing SMCs (0.142 ± 0.016 vs. 0.090 ± 0.011 μm^2; $P = 0.0012$, $n = 45$ nuclei/group) (Fig. 2*B*). An abnormal lamin B1 meshwork was restricted to cells with a morphologically abnormal progerin meshwork. Also, the sizes of the openings in the lamin B1 meshwork were virtually identical to those in the progerin meshwork (Fig. 2*D*).

Nonfarnesyl-progerin did not alter the structure of the lamin B1 meshwork (Fig. 2 *A* and *B*). Much of the nonfarnesyl-progerin was in the nucleoplasm (*SI Appendix*, Fig. S1 *B–D*), but some of it was located at the nuclear rim (colocalizing with lamin B1 and LAP2β) (*SI Appendix*, Fig. S1 *B–D*). The nonfarnesyl-progerin along the nuclear rim formed a regular meshwork with small openings (Fig. 2*A*).

We used a lamin C–specific antibody to define the distribution of endogenous lamin C. [The lamin C–specific antibody was validated by western blotting and immunocytochemistry (*SI Appendix*, Fig. S2).] Lamin C staining in wild-type SMCs had a punctate pattern, both at the nuclear rim and in the nucleoplasm (Fig. 3 *A* and *B*). While the staining was predominantly punctate, in some cases lamin C appeared to line one or two sides of an opening in the lamin A meshwork. In progerin-expressing cells, lamin C puncta bordered openings in the progerin meshwork, including in regions of the meshwork containing large gaps and irregularities (Fig. 3*B*).

NM Ruptures and Nuclear Blebs Are Associated with an Abnormal Progerin Meshwork. Progerin triggers nuclear blebs and NM ruptures in SMCs (21). We suspected that the ruptures and blebs were associated with abnormalities in the progerin meshwork. To test that suspicion, progerin-expressing SMCs were fixed and stained with a human lamin A–specific antibody. Cells with nuclear blebs ($n = 171$) and without nuclear blebs ($n = 132$) were identified on low-magnification images and then characterized further by high-resolution confocal microscopy (Fig. 4*A*). Nuclear blebs and an abnormal progerin meshwork were strongly correlated; 71% of cells with a nuclear bleb had an abnormal progerin meshwork, whereas only 14% of cells without a bleb exhibited an abnormal meshwork (Fig. 4*B*). Similar analyses were performed for NM ruptures. NM ruptures were identified by live-cell imaging in progerin-SMCs that expressed a nuclear-targeted green fluorescent protein reporter (nls-GFP) (19, 27). NM ruptures were identified by leakage of nls-GFP into the cytoplasm (Fig. 4*C*). After 48 h of imaging, the cells were fixed and examined by immunofluorescence confocal microscopy. An abnormal progerin meshwork was observed in 72% of cells with a NM rupture ($n = 120$) but in only 16% of cells without a NM rupture ($n = 273$) (Fig. 4*D*). Nuclear blebs and NM ruptures were also strongly correlated; 84% of cells

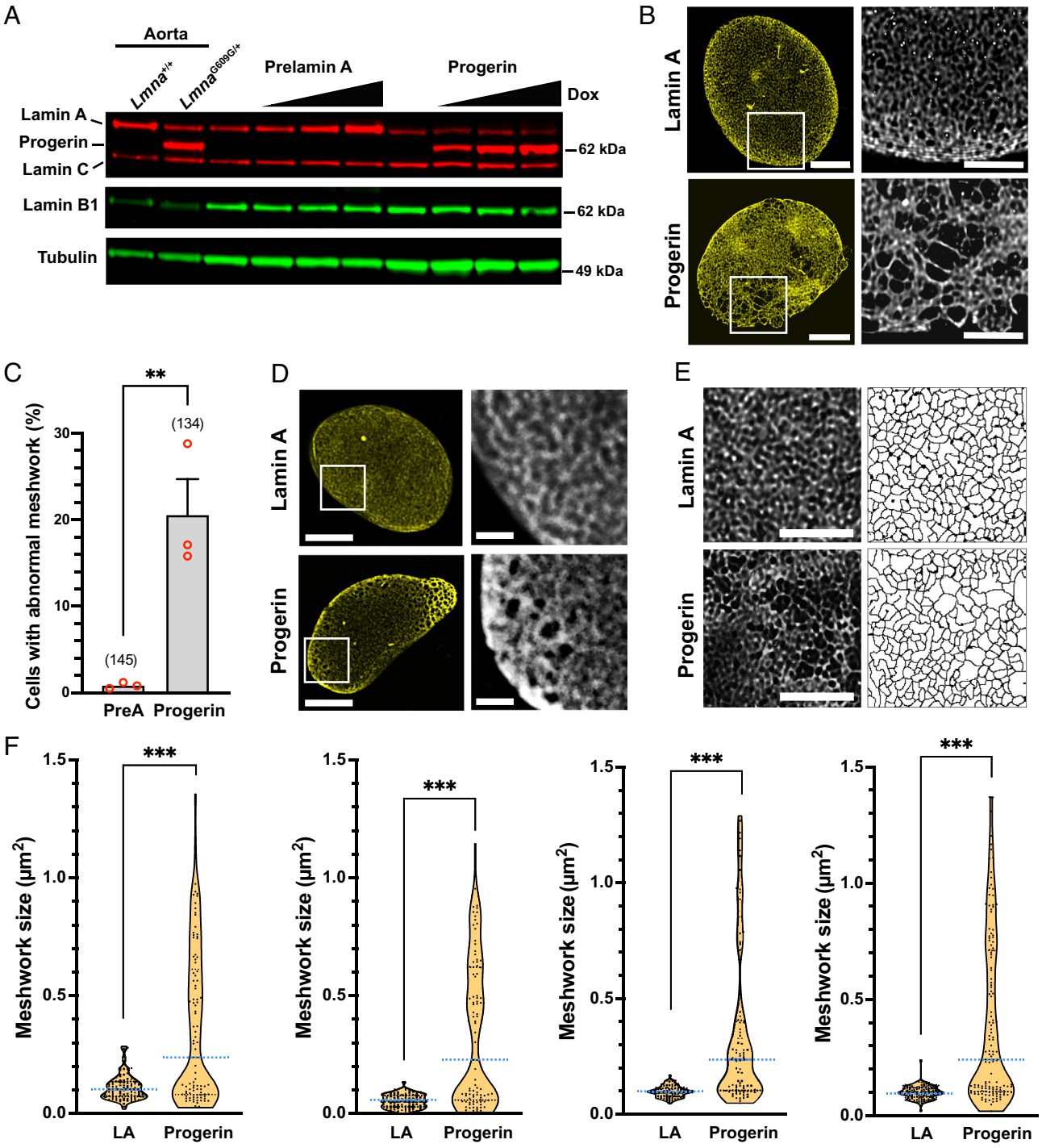

Fig. 1. The nuclear lamin meshwork is abnormal in progerin-expressing SMCs. (*A*) Western blot comparing the expression of lamin A and progerin in the mouse aorta and in cultured SMCs expressing Dox-inducible constructs for human (hu)-prelamin A and hu-progerin. Tubulin was measured as a loading control. (*B*) Confocal fluorescence microscopy images of the lamin A (*Upper*) and progerin (*Lower*) meshworks in SMCs stained with an antibody against hu-lamin A (yellow). High-magnification images of the boxed regions are shown to the *Right*. (Scale bar, 2 μm.) (*C*) The percentage of cells with an abnormal nuclear lamin meshwork in SMCs expressing prelamin A (PreA) or progerin. The total numbers of cells examined in three independent experiments (circles) are shown in parentheses. Mean ± SEM. $^{**}P < 0.01$. (*D*) STED microscopy images of the lamin A (*Upper*) and progerin (*Lower*) meshworks in SMCs stained with an antibody against hu-lamin A (yellow). High-magnification images of the boxed regions are shown to the *Right*. (Scale bar, 1 μm.) (*E*) Representative microscopy images (*Left*) and line drawings (*Right*) of 4 × 4-μm regions in the lamin A (*Upper*) and progerin (*Lower*) meshworks in SMCs. (Scale bar, 2 μm.) (*F*) Violin plots comparing the distribution (tan) and average sizes (mean; blue dotted lines) of the openings in the lamin A (PreA) and progerin meshworks in four pairs of nuclei. $^{***}P < 0.001$.

with a NM rupture had a nuclear bleb (Fig. 4*E*), and 91% of cells with a nuclear bleb had a NM rupture (Fig. 4*F*).

An Abnormal Progerin Meshwork in Nuclear Blebs Is Associated with Low Lamin B1 Levels. We stained progerin-expressing SMCs with antibodies against human lamin A (to detect progerin), lamin B1, and LAP2β and then imaged cells with nuclear blebs by high-resolution confocal microscopy. Nuclear blebs contained both progerin and LAP2β, and the intensity of progerin and LAP2β staining in blebs was similar to that along the nuclear rim (Fig. 5*A*). In contrast, lamin B1 staining of blebs was heterogenous. In ~50% of nuclear blebs, lamin B1 expression was barely detectable (Fig. 5 *A* and *B*). Maximum intensity projections confirmed low amounts of lamin B1 expression in the bleb relative to amounts

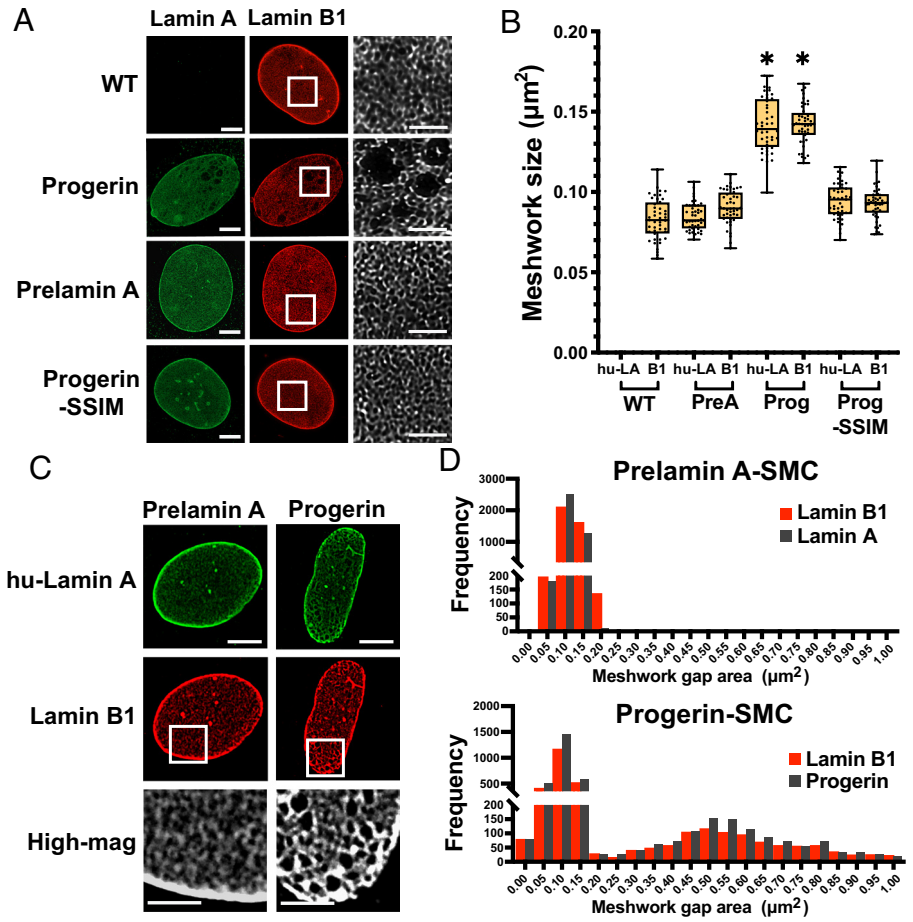

Fig. 2. Progerin has a dominant-negative effect on the structure of the lamin B1 meshwork. (*A*) Representative confocal fluorescence microscopy images of wild-type SMCs (WT) and SMCs expressing hu-progerin, hu-prelamin A, and hu-progerin-SSIM. Cells were stained with antibodies against hu-lamin A (green) and lamin B1 (red). (Scale bar, 2.5 μm.) High-magnification images of the boxed regions are shown to the *Right*. (Scale bar, 2 μm.) (*B*) Box and whisker plots comparing the average sizes (mean; solid black line inside box) and ranges of the openings in the meshworks of WT SMCs, and SMCs expressing hu-prelamin A (hu-PreA), hu-progerin (hu-Prog), and hu-Prog-SSIM. The cells were stained with antibodies against hu-lamin A and mouse lamin B1. Mean ± SEM. *$P < 0.05$ ($n = 45$ nuclei/group) compared to SMCs expressing prelamin A. (*C*) STED microscopy images of SMCs expressing prelamin A (*Left*) or progerin (*Right*) stained with antibodies against hu-lamin A (green) and lamin B1 (red). (Scale bar, 5 μm.) High-magnification images of the boxed regions are shown at the *Bottom*. (Scale bar, 1.0 μm.) (*D*) Bar graphs showing the sizes of the openings in the lamin A (black) and lamin B1 (red) meshworks in SMCs expressing hu-prelamin A (*Top*) and the progerin (black) and lamin B1 (red) meshworks in SMCs expressing hu-progerin (*Bottom*). A break in the *Y*-axis was used to optimize viewing of the sizes of lower-frequency openings in the meshwork.

at the nuclear rim. In blebs with very low levels of lamin B1, the progerin meshwork was irregular with large openings (Fig. 5*C*). The irregular pattern was observed in 96% of blebs with low levels of lamin B1 ($n = 98$ cells). In contrast, only 3% of blebs with strong lamin B1 staining had a morphologically abnormal progerin meshwork ($n = 102$ cells) (Fig. 5*D*).

Nuclear Blebs Form at Sites of NM Ruptures. We observed a strong association between NM ruptures and nuclear blebs in progerin-expressing SMCs (Fig. 4*F*). To understand that association, we used live-cell imaging to monitor bleb formation and NM ruptures in progerin-expressing SMCs that expressed nls-GFP and cGAS-mCherry [to mark NM rupture sites; (28, 29)]. After Dox-induction of progerin expression, the frequency of nuclear blebs and NM ruptures increased. After 48 h, 14% of the cells had a nuclear bleb or a NM rupture (Fig. 6*A*). Consistent with earlier studies (27, 30), NM ruptures occurred more frequently in cells with nuclear blebs (Fig. 6*B*). Of note, cGAS-mCherry was often found in nuclear blebs (Fig. 6*C* and Movie S1), suggesting that blebs formed at a NM rupture site. Indeed, live-cell imaging revealed that 81% of new blebs formed at a NM rupture site (Fig. 6*D*). Because progerin causes repetitive NM ruptures in SMCs (21) and because NM ruptures are more frequent in cells with a nuclear bleb (Fig. 6*B*), we suspected that we would find NM ruptures within blebs. Indeed, we observed NM ruptures (as judged by cGAS-mCherry labeling) at a nuclear bleb, which was associated with the formation of smaller blebs within the nuclear bleb (Fig. 6*E*).

Because we had previously documented NM ruptures in vivo in aortic SMCs of $Lmna^{G609G}$ mice (21), we predicted that we might also encounter nuclear blebs in aortic SMCs. Indeed, we found nuclear blebs in SMCs in the aorta of 10-wk-old $Lmna^{G609G/G609G}$ mice (Fig. 6*F* and *SI Appendix*, Fig. S3*B*). In some of those cells, we observed (with a lamin A/C–specific antibody) an abnormal nuclear lamina meshwork (Fig. 6*F* and *SI Appendix*, Fig. S3*B*).

NM Ruptures and Nuclear Blebs Are Associated with an Abnormal Nuclear Lamin Meshwork in $Lmnb1^{-/-}$ and $Zmpste24^{-/-}$ SMCs. To further explore the relationship between nuclear blebs and NM ruptures, we created $Zmpste24^{-/-}$ and $Lmnb1^{-/-}$ SMCs. Immunocytochemistry studies identified increased nuclear blebs in $Zmpste24^{-/-}$ and $Lmnb1^{-/-}$ cells (*SI Appendix*, Fig. S4), and live-cell imaging revealed increased NM ruptures (Fig. 7*A*). At the end of the live-cell imaging, the SMCs were fixed and stained with antibodies against lamin A/C (to identify cells with a nuclear bleb)

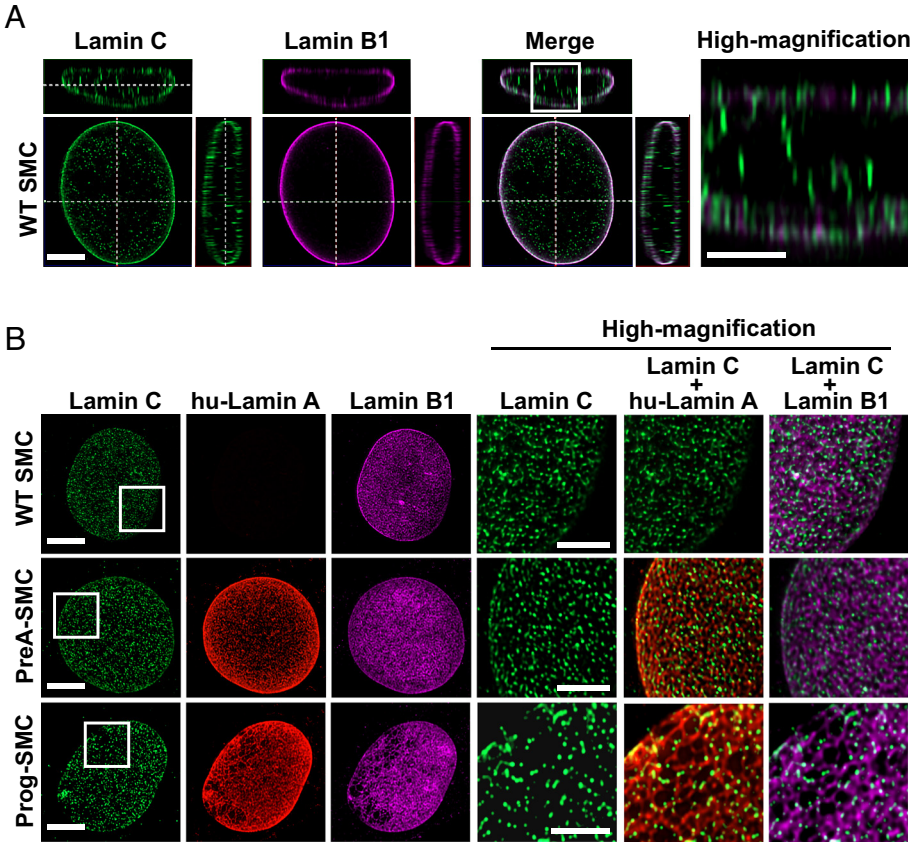

Fig. 3. Lamin C in progerin-SMCs is present along the borders of openings in the progerin meshwork. (*A*) Orthogonal views of a nucleus from a wild-type SMC (WT SMC) stained with antibodies against lamin C (green) and lamin B1 (magenta). Lamin C is located at the nuclear rim and in the nucleoplasm. (Scale bar, 5 μm.) A high-magnification image of the boxed region is shown to the *Right*. (Scale bar, 2 μm.) (*B*) Representative confocal fluorescence microscopy images of nuclei from WT-SMCs and SMCs expressing hu-prelamin A (PreA-SMC) and hu-progerin (Prog-SMC). Cells were stained with antibodies against lamin C (green), hu-lamin A (red), and lamin B1 (magenta). (Scale bar, 5 μm.) High-magnification images of the boxed areas are shown to the *Right*. (Scale bar, 2 μm.)

and cGAS (to identify NM rupture sites). In both *Zmpste24*$^{-/-}$ and *Lmnb1*$^{-/-}$ cells, NM ruptures were strongly correlated with blebs. In *Zmpste24*$^{-/-}$ cells with a bleb (n = 126 cells), 69% had a NM rupture. In *Zmpste24*$^{-/-}$ cells without a nuclear bleb (n = 187 cells), only 8% had a NM rupture (Fig. 7*B*). In *Lmnb1*$^{-/-}$ cells with a nuclear bleb (n = 174 cells), 91% had a NM rupture; in *Lmnb1*$^{-/-}$ cells without a nuclear bleb (n = 145 cells), 27% had a NM rupture (Fig. 7*B*).

Irregular lamin A meshworks with large gaps were identified in both *Lmnb1*$^{-/-}$ and *Zmpste24*$^{-/-}$ SMCs (Fig. 7*C*). In *Zmpste24*$^{-/-}$ cells with a nuclear bleb (n = 110 cells), 61.2% had an abnormal lamin A meshwork; in cells without a bleb (n = 198 cells), 2.5% had an abnormal lamin A meshwork (Fig. 7*D*). In *Lmnb1*$^{-/-}$ cells with a nuclear bleb (n = 156), 90.2% had an abnormal lamin A meshwork; in cells without a nuclear bleb (n = 129), 43.9% had an abnormal lamin A meshwork (Fig. 7*D*).

Lamin B1 and LAP2β Expression Normalized the Meshwork in Progerin-SMCs and Reduced the Frequency of Nuclear Blebs and NM Ruptures. The observation that lamin B1 levels were low in nuclear blebs that exhibited a structurally abnormal progerin meshwork led us to hypothesize that increased lamin B1 expression would normalize the morphology of the progerin meshwork. To test that hypothesis, we generated SMCs that expressed progerin constitutively and then introduced Dox-inducible constructs for lamin B1, nonfarnesyl–lamin B1, or HA-tagged LAP2β. Dox levels were adjusted to increase endogenous levels of lamin B1 and LAP2β by approximately threefold (*SI Appendix*, Fig. S5 *A* and *B*). After 48 h, cells were stained with antibodies against lamin A/C and lamin B1, and the nuclear lamin meshworks were examined by immunofluorescence confocal microscopy. Lamin B1 expression normalized the progerin meshwork (Fig. 8*A*), reducing the percentage of cells with an abnormal progerin meshwork from 20 to 4% (n = 86 to 114 cells/group in three independent experiments) (Fig. 8*B*). Nonfarnesyl–lamin B1 had no effect on the frequency of abnormal progerin meshworks (P = 0.57). Of note, LAP2β also reduced the percentage of cells with an abnormal progerin meshwork from 20 to 4% (Fig. 8*B*). High-resolution imaging of LAP2β in wild-type and progerin-SMCs revealed a uniform net-like staining pattern similar to that of the nuclear lamins (*SI Appendix*, Fig. S5 *C* and *D*).

Increased lamin B1 and LAP2β expression reduced the frequency of NM ruptures and blebs in progerin-expressing SMCs, consistent with their ability to improve the morphology of the progerin meshwork. Live-cell imaging studies revealed that lamin B1 and LAP2β reduced the percentage of progerin-expressing cells with NM ruptures from 20 to <6% (Fig. 8*C*) and reduced the frequency of nuclear blebs from ~16 to <4% (Fig. 8*C*). Nonfarnesyl–lamin B1 had no effect on the frequency of NM ruptures or blebs (Fig. 8*C*).

Discussion

Lamin A, an intermediate filament protein, is a major component of the nuclear lamina. Lamin A dimers assemble into head-to-tail protofilaments and then into higher-order filaments to form a fibrillar meshwork that lines the inner NM (31). Half-normal amounts of lamin A synthesis (*LMNA* haploinsufficiency) cause

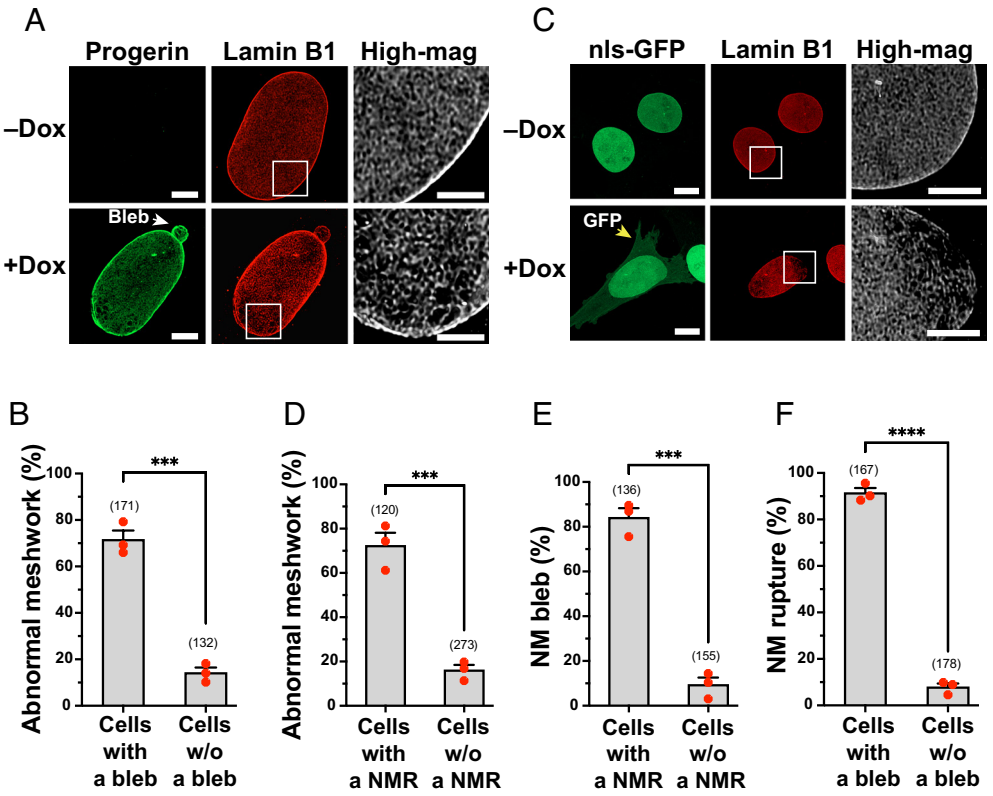

Fig. 4. NM ruptures and nuclear blebs are associated with an abnormal progerin meshwork. (*A*) Representative confocal fluorescence microscopy images of noninduced (–Dox) and induced (+Dox) progerin-SMCs stained with antibodies against hu-lamin A (green) and lamin B1 (red). (Scale bar, 5 μm.) Boxed regions are shown at higher magnification to the *Right*. (Scale bar, 2 μm.) The arrow points to a nuclear bleb. (*B*) Percentage of progerin-SMCs with a nuclear bleb that have an abnormal progerin meshwork. The total numbers of cells examined in three different experiments (circles) are shown in parentheses. Mean ± SEM. ***$P < 0.001$. (*C*) Representative confocal fluorescence microscopy images of noninduced (–Dox) and induced (+Dox) progerin-SMCs expressing nls-GFP (green) and stained with an antibody against lamin B1 (red). (Scale bar, 5 μm.) Boxed regions are shown at higher magnification to the *Right*. (Scale bar, 2 μm.) A cell with a NM rupture was identified by nls-GFP in the cytoplasm (yellow arrow). (*D*) Percentage of progerin-SMCs with a NM rupture (NMR) and an abnormal progerin meshwork. The total numbers of cells examined in three independent experiments (circles) are shown in parentheses. Mean ± SEM. ***$P < 0.001$. (*E*) Percentage of progerin-SMCs with a NMR that had a nuclear bleb. The total numbers of cells examined in three independent experiments (circles) are shown in parentheses. Mean ± SEM. ***$P < 0.001$. (*F*) Percentage of progerin-SMCs with a nuclear bleb that had a NMR. The total numbers of cells examined in three independent experiments (circles) are shown in parentheses. Mean ± SEM. ****$P < 0.0001$.

muscular dystrophy and cardiomyopathy in humans and mice (32, 33). A distinct genetic disease, HGPS, is caused by a de novo *LMNA* point mutation that leads to the production of progerin—an internally truncated lamin A containing a farnesyl lipid anchor. In children with HGPS, progerin causes disease in multiple tissues and does so despite production of lamin A from the unaffected *LMNA* allele. The ability of progerin to trigger severe disease—despite ongoing lamin A synthesis—prompted speculation that progerin exerts a dominant-negative effect on the nuclear lamina (1). Thus far, however, the mechanisms by which progerin causes disease have remained unclear. In the current study, our efforts to characterize the impact of progerin on the structure of the nuclear lamina uncovered fresh insights. We used mouse SMCs as a model system to better understand the mechanisms responsible for the progerin-induced NM ruptures and SMC loss in the aorta of $Lmna^{G609G}$ mice (21). High-resolution confocal microscopy of cultured SMCs revealed that lamin A and lamin B1 form similar but distinct meshworks—consistent with earlier studies (11, 12). We found that the two meshworks were similar in appearance but that the precise location of the fibrils and the openings in the meshworks differed. We showed that the expression of prelamin A in SMCs results in the formation of an orderly lamin A meshwork with very small openings. In contrast, progerin resulted in the formation of an irregular meshwork with clusters of large openings. Unexpectedly, progerin expression also resulted in an abnormal lamin B1 meshwork with large openings (corresponding to openings in the progerin meshwork), suggesting that progerin exerts a dominant-negative effect on the structure of the nuclear lamina. We suspect that progerin's capacity to affect the structure of the lamin B1 meshwork reflects direct protein–protein interactions between the two meshworks, or alternatively, the formation of mixed heteropolymers containing both lamin B1 and progerin (34).

Similar abnormalities in the progerin and lamin B1 meshworks in progerin-expressing SMCs were associated with a markedly increased frequency of NM ruptures and nuclear blebs. We found that increasing lamin B1 expression in progerin-expressing cells normalized the morphology of both the progerin and lamin B1 meshworks and resulted in a markedly reduced frequency of NM ruptures and blebs. In earlier studies (21), we found that increased lamin B1 expression in SMCs reduced progerin-induced nuclear stiffness, DNA damage, and cell death. Because progerin and lamin B1 both contain C-terminal modifications (i.e., farnesylation, carboxyl methylation) that promote their association with the inner NM (35, 36), we proposed that lamin B1 and progerin could compete for a limited number of binding sites at the nuclear rim (21). We further proposed that increasing lamin B1 expression reduces progerin's association with the inner NM and thereby reduces its toxicity. In support of that proposal, nuclear extraction studies revealed that increased expression of lamin B1 reduces the amount of progerin in the NM fraction (21). Our current studies revealed that increased lamin B1 expression minimizes progerin

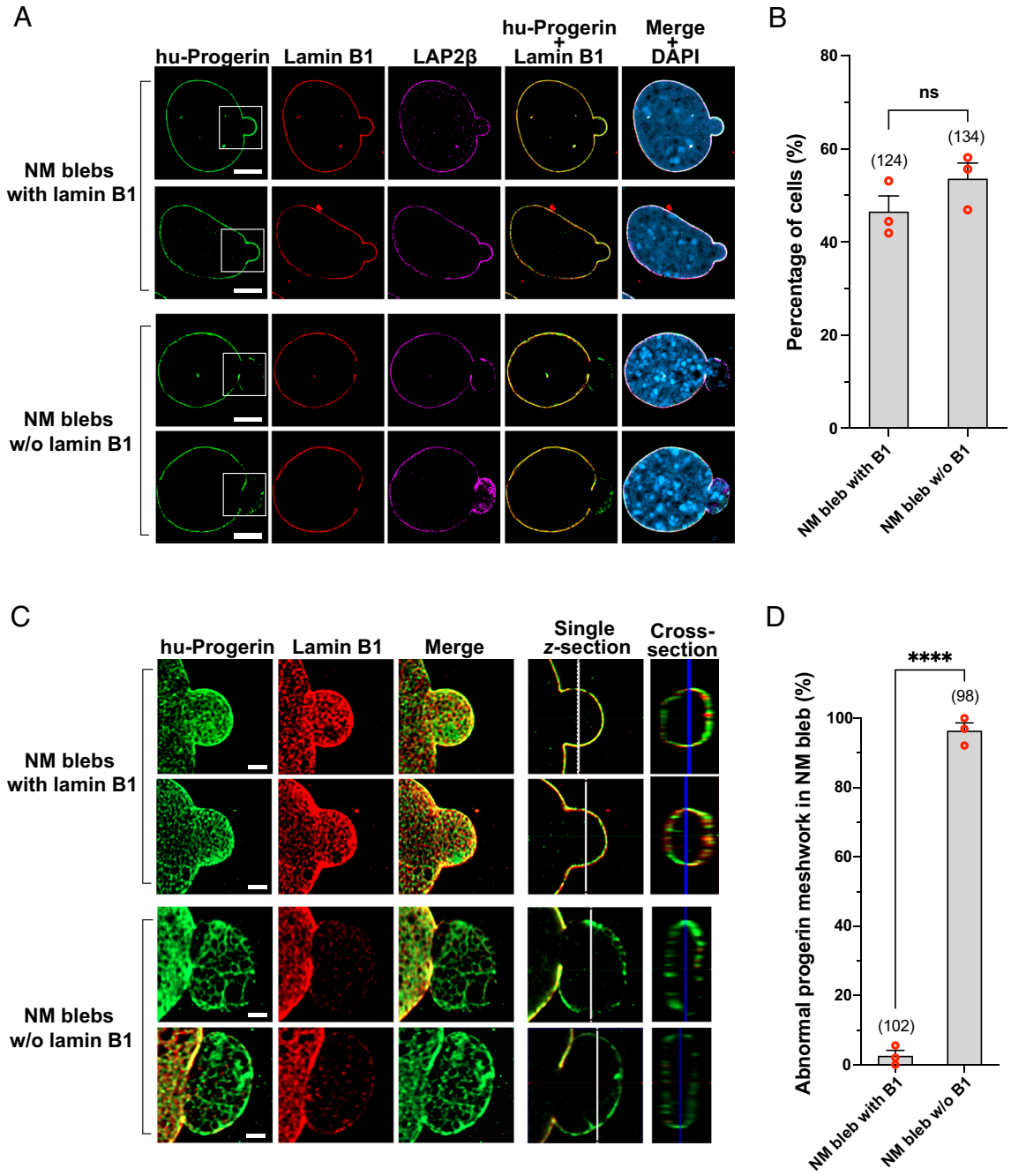

Fig. 5. An abnormal progerin meshwork in nuclear blebs is associated with low lamin B1 levels. (*A*) Representative confocal fluorescence microscopy images of progerin-SMCs stained with antibodies against hu-lamin A (green), lamin B1 (red), and LAP2β (magenta). DNA was stained with Dapi (blue). (Scale bar, 5 μm.) Single microscopy sections were collected through the middle of the nuclear bleb. The boxed areas are shown at higher magnification in panel *C*. (*B*) Percentage of nuclear blebs in progerin-SMCs with normal levels of lamin B1 or low levels of lamin B1. The total numbers of cells examined in three experiments (circles) are shown in parentheses. Mean ± SEM. ns, not significant. (*C*) High-resolution microscopy images of the progerin and lamin B1 meshworks in the nuclear blebs boxed in panel *A*. (Scale bar, 1 μm.) (*D*) Percentage of nuclear blebs with an abnormal progerin meshwork in blebs with lamin B1 and blebs without lamin B1. The total numbers of cells examined in three independent experiments (circles) are shown in parentheses. Mean ± SEM. ****$P < 0.001$.

toxicity (i.e., NM ruptures and blebs) by normalizing the progerin and lamin B1 meshworks. We suspect that the normalization of the meshworks is related, at least in part, to displacement of progerin from inner NM binding sites.

Our use of Dox-inducible vectors to express prelamin A and progerin was crucial; this approach allowed us to examine SMC clones that expressed equivalent amounts of lamin A and progerin. It is difficult to reproducibly achieve comparable expression levels with transiently transfected SMCs or "mixed stable" SMCs—or with studies with human fibroblast cell lines. In our current studies, we matched progerin levels in cultured SMCs to levels in the aortas of $Lmna^{G609G/+}$ mice. Lamin A levels in the aortas of $Lmna^{+/+}$ mice and progerin levels in the aortas of $Lmna^{G609G/+}$ mice are ~fourfold to fivefold higher than lamin C levels (25). We produced progerin-expressing SMC clones with a progerin:lamin C ratio of ~3:1. At those levels, we found morphological abnormalities in both the progerin meshwork and the lamin B1 meshwork. The use of the Dox-inducible expression system in SMCs held another advantage—aside from allowing us to fine-tune protein expression levels. Because the SMC clones were grown in Dox-free medium, we were able—by adding Dox to the medium—to examine the impact of progerin expression in naive SMCs. Had we performed

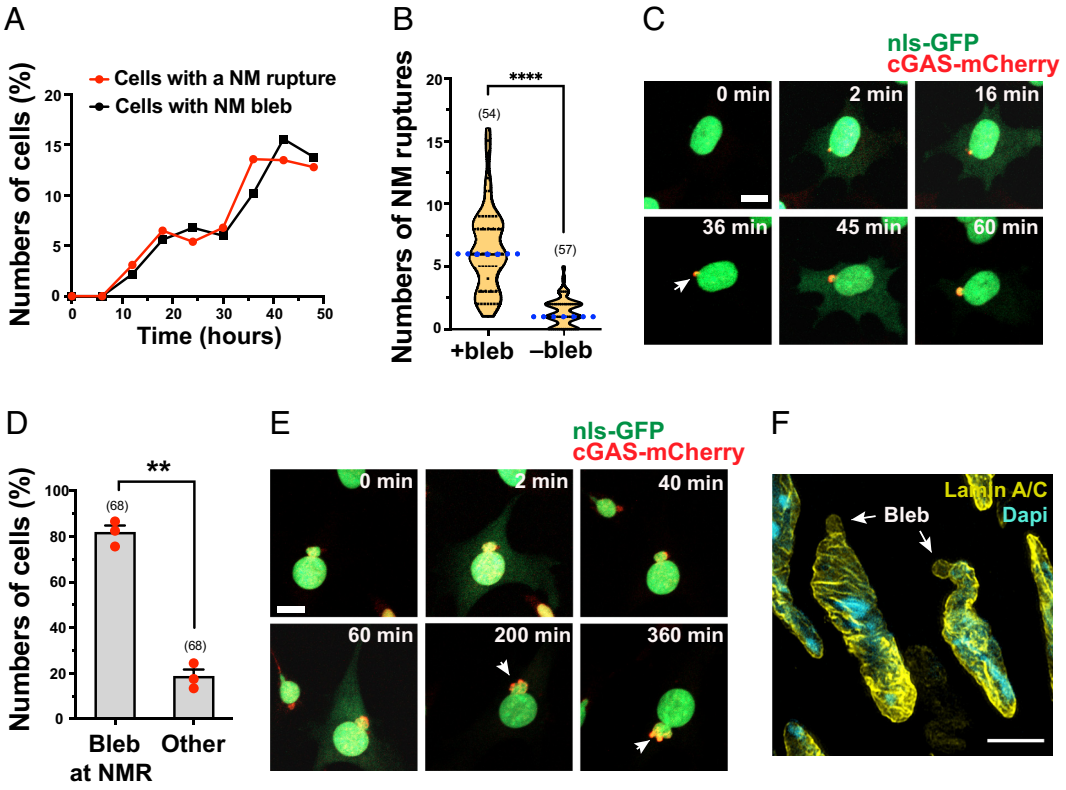

Fig. 6. Nuclear blebs form at sites of NM ruptures. (*A*) Kinetics of nuclear bleb formation (black squares) and NM ruptures (red circles) after adding Dox to induce progerin synthesis. (*B*) Frequency of NM ruptures in progerin-SMCs with a nuclear bleb and without a nuclear bleb. The total numbers of cells examined are shown in parentheses. Mean ± SD. ****$P < 0.0001$. (*C*) Still images from a live-cell recording (Movie S1) of progerin-SMCs expressing nls-GFP (green) and cGAS-mCherry (red). A NM rupture at 2 min (identified by the appearance of GFP in the cytoplasm) was followed by the formation of a nuclear bleb labeled with cGAS-mCherry (arrow). (Scale bar, 10 μm.) The time mark (relative to the first image) is shown in the *Upper Right*. (*D*) Bar graph showing the frequency of a nuclear bleb forming at a NM rupture (NMR) site. The total numbers of cells examined from three experiments (circles) are shown above each bar. Mean ± SEM. **$P < 0.01$. (*E*) Still images from a time-lapse video (Movie S2) of progerin-SMCs showing the formation of nuclear bleb on an existing bleb after a NM rupture. (Scale bar, 10 μm.) The arrow points to two small nuclear blebs that formed on a larger nuclear bleb. (*F*) Confocal fluorescence microscopy image of aortic SMCs from a 10-wk-old *Lmna*$^{G609G/G609G}$ mouse stained with an antibody against lamin A/C (yellow). DNA was stained with Dapi (blue). (Scale bar, 5 μm.) The arrows point to nuclear blebs.

studies in SMCs that expressed progerin constitutively, we would have needed to consider the long-term effects of progerin toxicity (e.g., DNA damage, cell senescence, altered gene expression) on the morphology of the nuclear lamina and on the frequency of NM ruptures and nuclear blebs.

In recent studies, Buxboim et al. (37) examined the nuclear lamina by cryoelectron tomography and reported that nuclear lamin filaments in progerin-expressing fibroblasts were more densely packed than in wild-type fibroblasts. While the cryo-electron microscopy (EM) studies could not identify which nuclear lamins contributed to increased filament density, they succeeded in showing that the nuclear lamina in progerin-expressing cells was morphologically distinct. Their finding of increased filament density is consistent with our finding that progerin expression results in morphologically abnormal progerin and lamin B1 meshworks.

The ability of progerin to induce morphological abnormalities in the nuclear lamin meshwork depended on progerin farnesylation. The expression of nonfarnesyl-progerin in SMCs resulted in a morphologically normal meshwork at the nuclear rim (colocalizing with lamin B1 and LAP2β), although a substantial fraction of nonfarnesyl-progerin was in the nucleoplasm. Consistent with an absence of disease phenotypes in knock-in mice expressing nonfarnesylated progerin (38), nonfarnesyl-progerin expression in SMCs did not increase the frequency of NM ruptures and blebs. We suspect that the ability of nonfarnesyl-progerin to reach the nuclear rim and form a morphologically normal meshwork was dependent on direct interactions with other nuclear lamins. Another reason to suspect that nonfarnesyl-progerin interacts with other nuclear lamins was the fact that nonfarnesyl-progerin triggered abnormalities in the distribution of lamin B1. In wild-type SMCs, lamin B1 is located at the nuclear rim, whereas in nonfarnesyl-progerin–expressing SMCs some of the lamin B1 was in the nucleoplasm, likely trapped there by interactions with nucleoplasmic nonfarnesyl-progerin. In any case, we suspect that the reduced toxicity of nonfarnesyl-progerin in SMCs results from its ability to form a regular meshwork and its inability to trigger NM ruptures and blebs.

When wild-type cells are incubated in medium containing a protein farnesyltransferase inhibitor (FTI), nonfarnesyl–prelamin A can be detected in the nucleoplasm and at the nuclear rim (7, 39). Similarly, when progerin-expressing cells are incubated with an FTI, nonfarnesyl-progerin can be detected in the nucleoplasm (7, 15, 39–41) and at the nuclear rim. Based in part on those findings, FTIs have been tested as a potential treatment for HGPS. In both human and mouse studies, FTIs were reported to reduce disease in mouse models of progeria (4, 42–44). In our studies with a gene-targeted HGPS mouse model, we found that adding an FTI to the drinking water resulted in modest short-term improvements in body weight and bony abnormalities, but the progression of disease was relentless and severe (4). Given current data, we believe that treatment of children with FTIs is reasonable. However, in considering FTIs as a therapeutic strategy, one must also consider the potential impact of the FTI on lamin B1 farnesylation. In our studies, we found that increased expression of wild-type (farnesyl-)lamin B1 in SMCs improved the morphology

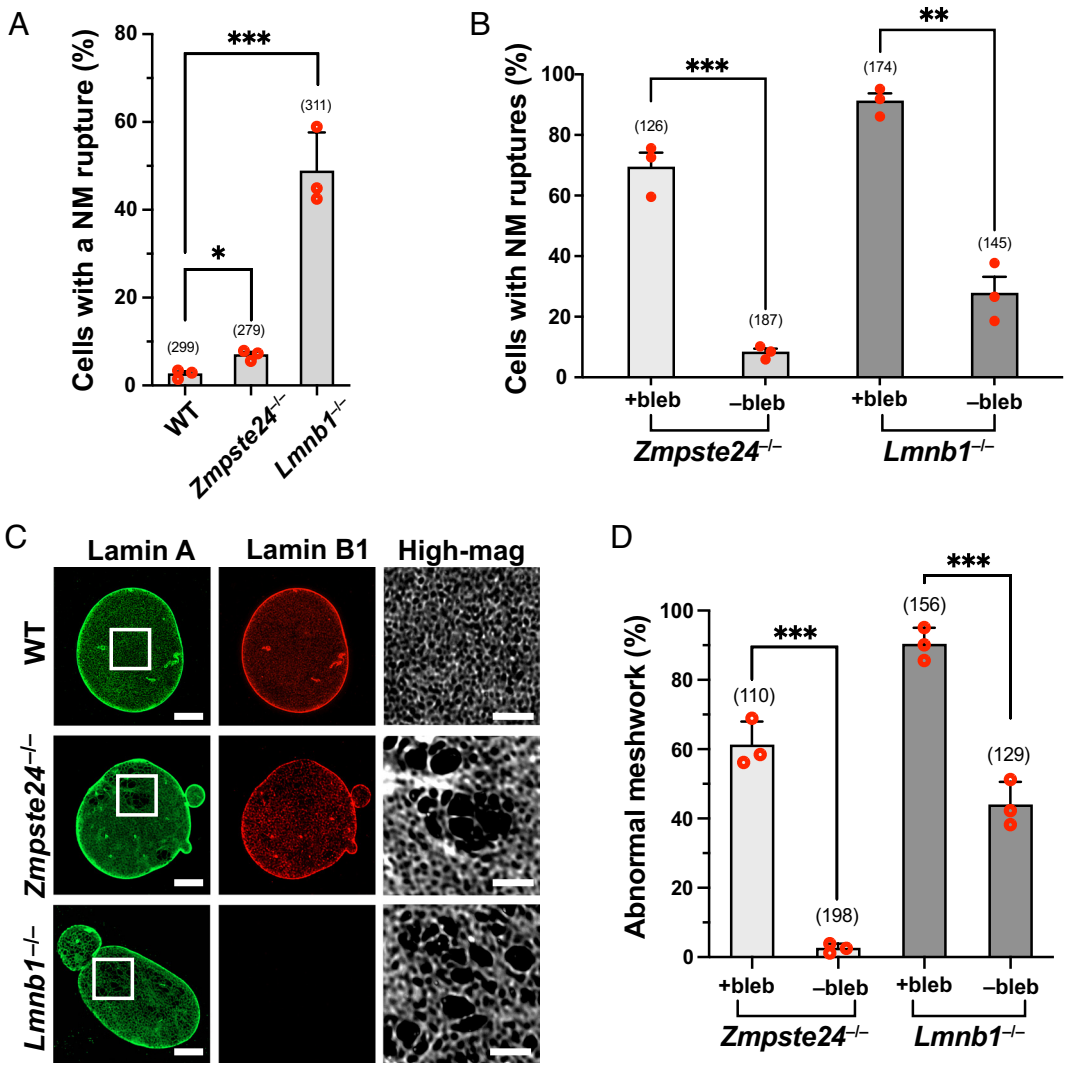

Fig. 7. NM ruptures and nuclear blebs are associated with an abnormal nuclear lamin meshwork in *Lmnb1*$^{-/-}$ and *Zmpste24*$^{-/-}$ SMCs. (*A*) Bar graph showing the percentage of cells with a NM rupture in wild-type (WT), *Zmpste24*$^{-/-}$, and *Lmnb1*$^{-/-}$ SMCs. The total numbers of cells examined in three independent experiments (circles) are shown in parentheses. Mean ± SEM. *$P < 0.05$; ***$P < 0.001$. (*B*) Bar graph showing the frequency of NM ruptures in *Zmpste24*$^{-/-}$ and *Lmnb1*$^{-/-}$ SMCs with and without a nuclear bleb. The total numbers of cells examined in three independent experiments (circles) are shown in parentheses. Mean ± SEM. **$P < 0.01$; ***$P < 0.001$. (*C*) Representative high-resolution microscopy images of cells stained with antibodies against lamin A (green) and lamin B1 (red) in WT, *Zmpste24*$^{-/-}$, and *Lmnb1*$^{-/-}$ SMCs. (Scale bar, 5 μm.) Boxed areas are shown at higher magnification on the *Right*. (*D*) Bar graph showing the frequency of an abnormal lamin A meshwork in *Zmpste24*$^{-/-}$ and *Lmnb1*$^{-/-}$ SMCs with and without a nuclear bleb. The numbers of cells scored in three independent experiments (circles) are shown in parentheses. Mean ± SEM. ***$P < 0.001$.

of the progerin meshwork and reduced the frequency of NM ruptures and blebs. In contrast, a comparable amount of nonfarnesyl-lamin B1 had no effect on the morphology of the progerin meshwork, nor did it reduce the frequency of NM ruptures and blebs. Thus, inhibiting the farnesylation of progerin with an FTI could minimize the toxicity of progerin, but it seems possible that any salutary effects of the drug could be blunted by inhibition of lamin B1 farnesylation [assuming that lamin B1 is not alternatively prenylated; (45)].

In our studies, we examined, by confocal microscopy, the distribution of lamin C in prelamin A–expressing and progerin-expressing SMCs. The lamin C antibody that we used was specific; there was no binding of the antibody to *Lmna*$^{-/-}$ cells, nor was there any binding of the antibody to other nuclear lamins on western blots. In WT SMCs, prelamin A–expressing SMCs and progerin-expressing SMCs, the distribution of lamin C was predominantly punctate. Lamin C puncta were found immediately adjacent to lamin A, progerin, and lamin B1 fibrils within the nuclear lamin meshworks. Occasionally, lamin C lined one or more sides of small openings in a nuclear lamin meshwork, but we were not able to detect a net-like meshwork resembling the meshworks formed by lamin A, progerin, or lamin B1. We suspect that this result is due low amounts of lamin C within cells (46) or perhaps to reduced binding of the lamin C–specific antibody to fixed samples. In any case, we speculate that lamin C does form an independent meshwork, and in the setting of progerin expression, we predict that lamin C forms an abnormal meshwork akin to the morphologically abnormal lamin B1 meshwork in progerin-expressing SMCs.

In earlier studies (13), we found that overexpression of an inner NM protein, LAP2β, eliminated NM ruptures in *Lmna*$^{-/-}$ *Lmnb1*$^{-/-}$*Lmnb2*$^{-/-}$ fibroblasts. In the current studies, we found that expression of LAP2β in progerin-expressing SMCs normalized the morphology of the progerin meshwork—and did so as effectively as lamin B1. Like lamin B1, LAP2β expression reduced the frequency of nuclear blebs and ruptures. The mechanism by which LAP2β normalizes the progerin meshwork is not understood, but our confocal microscopy studies showed that LAP2β adopts a net-like pattern resembling the lamin A and lamin B1 meshworks. We suspect that the net-like distribution of LAP2β functions to normalize the progerin meshwork and minimize NM

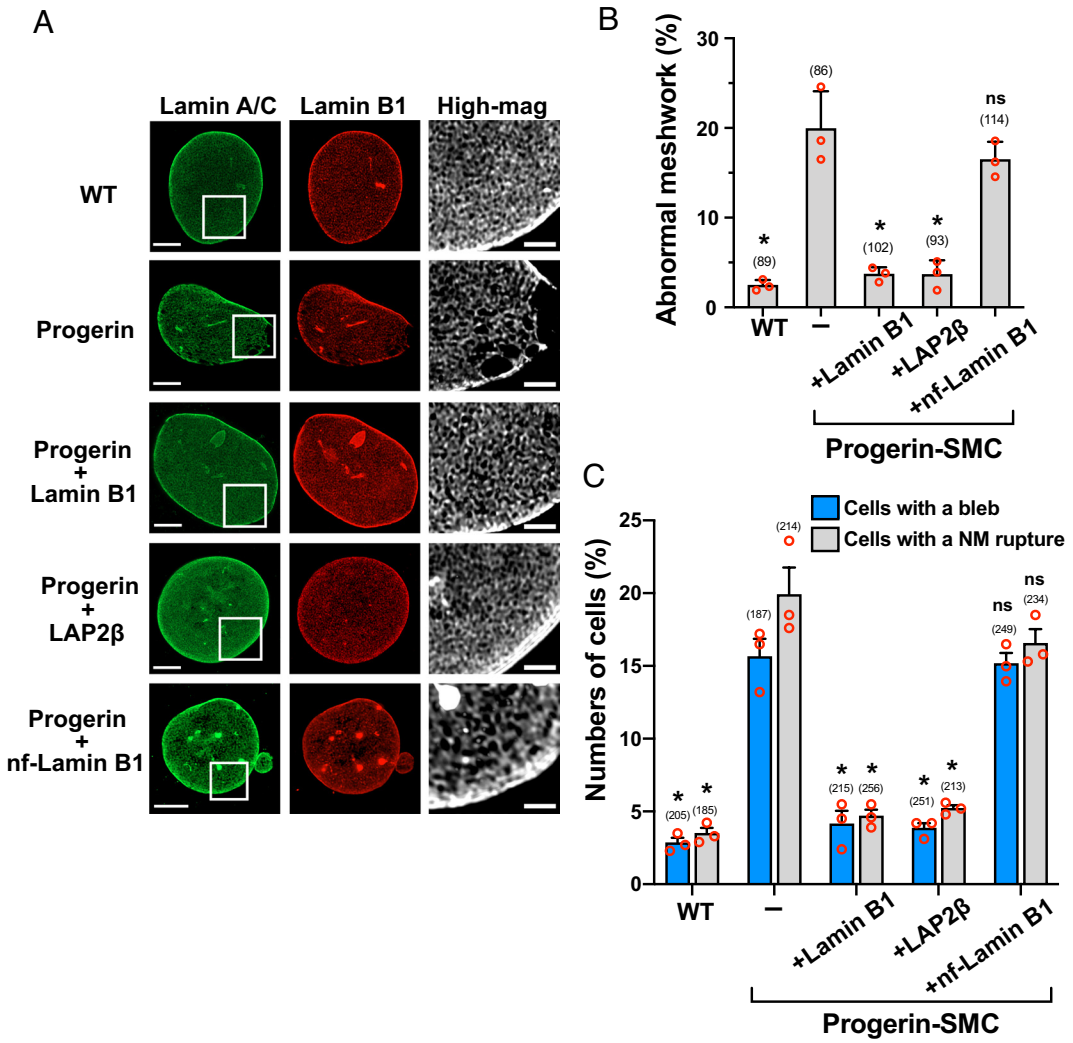

Fig. 8. Lamin B1 and LAP2β expression normalized the meshwork in progerin-SMCs and reduced the frequency of NM ruptures and nuclear blebs. (*A*) Representative high-resolution microscopy images of WT SMCs, and SMCs expressing progerin, progerin + lamin B1, progerin + LAP2β, or progerin + nonfarnesyl-lamin B1 (nf-lamin B1); cells were stained with antibodies against lamin A/C (green) and lamin B1 (red). High-magnification images of the boxed regions are shown on the right (white). (Scale bar, 5 μm.) (*B*) Percentage of cells with an abnormal nuclear lamin meshwork in WT-SMCs, progerin-SMCs, and progerin-SMCs expressing lamin B1, LAP2β, or nf-lamin B1. The numbers of cells examined in three independent experiments (circles) are shown in parentheses. Mean ± SEM. **P* < 0.05. One-way ANOVA showing comparisons to progerin-SMCs. (*C*) Percentage of cells with a nuclear bleb (blue) or NM rupture (gray) in WT-SMCs, progerin-SMCs, and progerin-SMCs expressing lamin B1, LAP2β, or nf-lamin B1. The numbers of cells examined in three independent experiments (circles) are shown in parentheses. Mean ± SEM. **P* < 0.05. Two-way ANOVA showing comparisons to progerin-SMCs. ns, not significant.

ruptures and blebs. The nucleoplasmic domain of LAP2β has been reported to interact with nuclear lamins, in particular lamin B1, but it is unclear whether that property is responsible for LAP2β's net-like distribution or its capacity to improve the morphology of the progerin network. It is interesting that the nucleoplasmic portion of emerin (an inner NM protein related to LAP2β) forms filamentous structures in vitro (47), but thus far there have been no reports that LAP2β shares that property.

Our studies are consistent with earlier studies showing that NM ruptures are more frequent in cells with a nuclear bleb (27, 30), presumably due to a weakened nuclear envelope (28). In our studies, we found, with live-cell imaging studies, that ~80% of new nuclear blebs in progerin-expressing SMCs form at a NM rupture site, explaining the strong correlation between NM ruptures and blebs. NM ruptures occurred more frequently in progerin-expressing cells with an abnormal meshwork, suggesting that the irregularities and large openings in the meshwork weakened the nuclear lamina and were causally related to the emergence of NM ruptures and blebs. In *Zmpste24*$^{-/-}$ and *Lmnb1*$^{-/-}$ SMCs, we also observed a very strong association between NM ruptures, nuclear blebs, and irregularities and gaps in the nuclear lamin meshworks. Those observations provided additional support for the notion that a weakened, structurally abnormal meshwork contributes to NM ruptures and bleb formation.

Increasing lamin B1 expression in progerin-expressing SMCs counteracted the impact of progerin on the structure of the nuclear lamina and reduced the frequency of nuclear blebs and ruptures. We suspect that lamin B1's capacity to mitigate progerin-induced phenotypes in SMCs is physiologically relevant, with high levels of lamin B1 in tissues protecting against disease and low levels increasing the severity of disease. In this context, we have been intrigued by a hallmark histopathologic finding in HGPS—loss of SMCs in the medial layer of the aorta (26). In wild-type mice, the lamin A:lamin B1 ratio is extremely high in the aorta (the highest among a comparison of 13 tissues, including bone and skin) (25). In the setting of progerin expression in *Lmna*$^{G609G/+}$ mice, where progerin protein accumulates with age while lamin B1 levels fall, the progerin:lamin B1 ratio in the aorta rises to very high levels; the progerin:lamin B1 ratio in the aorta is ~25 to 30 (relative to the kidney set at 1), whereas it is only ~2.5 in left

ventricular myocardium (25). We suspect that the low amounts of lamin B1 render progerin-expressing SMCs more susceptible to progerin toxicity, resulting in an abnormal progerin meshwork and an increased susceptibility to mechanical stress associated with pulsatile blood flow. In support of that proposal, we found an abnormal lamin A/C meshwork in aortic SMCs of *Lmna*$^{G609G/G609G}$ mice. The arterial pathology in mouse HGPS is restricted to medial SMCs. We have never observed loss of intimal endothelial cells or adventitial mesenchymal cells even though the intima and adventitia are also exposed to mechanical stress. We suspect that the substantially higher amounts of lamin B1 in intimal and adventitial cells (25) render them less susceptible to disease.

Materials and Methods

Mice. Mice with a targeted HGPS mutation (*Lmna*^{G609G}) (25, 48) were housed in a specific pathogen–free barrier facility with a 12-h light/dark cycle. The mice were provided pelleted mouse chow (NIH31) and water ad libitum and nutritional food cups (Westbrook, ME) as required for supportive care. All animal studies were approved by UCLA's Animal Research Committee.

***Lmnb1*-Deficient SMCs.** Guide RNAs targeting *Lmnb1*-deficient SMCs (*Lmnb1*$^{-/-}$) (lacking any detectable lamin B1 by western blot or immunocytochemical staining) were created by CRISPR/Cas9-induced homology-directed repair. A detailed description is provided in *SI Appendix*.

***Zmpste24*-Deficient SMC.** *Zmpste24*-deficient SMCs were created in a similar fashion as *Lmnb1*-deficient SMCS. A detailed description is provided in *SI Appendix*.

Western Blotting. Western blotting of cell and tissue samples was performed as previously described (21, 25). A description is provided in *SI Appendix*. The antibodies and concentrations are listed in *SI Appendix*, Table S1.

Quantitative Real-Time PCR. Quantitative real-time PCR was performed as previously described (21). A detailed description is provided in *SI Appendix*. All primers used in the experiments are listed in *SI Appendix*, Table S2.

Dox-Inducible Expression in SMCs. SMCs harboring Dox-inducible pTRIPZ expression vectors for human prelamin A, human progerin, nonfarnesylated human progerin (progerin-SSIM), lamin B1, and nonfarnesylated lamin B1 (lamin B1-SAIM) have been described previously (21, 25). A similar approach was used to generate SMCs expressing Dox-inducible constructs for LAP2β. A detailed description is provided in *SI Appendix*. The primer sequences are listed in *SI Appendix*, Table S3.

Constitutive Expression of Nuclear-Localized GFP, cGAS-mCherry, and Lamins in SMCs. SMCs expressing GFP with a nuclear localization signal (nls-GFP) have been described previously (21). The creation of SMCs expressing constitutive plasmids for prelamin A and progerin is described in *SI Appendix*.

Measurement of NM Ruptures in Live SMCs. The detection of NM ruptures was performed as previously described (21). A description is provided in *SI Appendix*.

High-Resolution Confocal Fluorescence Microscopy. A total of 50,000 cells were grown in a chambered coverslip with a #1.5H (170 μm ± 5 μm) glass bottom (ibidi USA). After 48 h, cells (with or without Dox) were fixed with 4% paraformaldehyde in PBS for 10 min at room temperature and permeabilized with 0.3% Triton X-100 in PBS for 10 min. The cells were processed for immunofluorescence microscopy as described (21). The antibodies and concentrations are listed in *SI Appendix*, Table S1. The settings for the collection of images by high-resolution microscopy and STED microscopy are described in detail in *SI Appendix*.

Quantification of Lamina Meshwork Gap. *Z*-axis images from 0.28 μm (the thickness of two *Z*-sections) above the equatorial plane to the top of the nucleus were compiled and converted to 8-bit grayscale with ImageJ (NIH). This strategy prevents overshadowing the meshwork morphology at the nuclear periphery. Brightness and contrast were adjusted to enhance the visibility of the lamina meshwork using ImageJ. The meshwork was outlined using the "Overlay" tool with a paintbrush set to a width of 1 pixel. A threshold was then applied to delineate the meshwork, and the area of the gaps within the meshwork was quantified with the "Analyze Particles" function. A global scale was established with a scale bar from the original image. Meshwork gaps adjacent to the image borders were excluded from quantification. The quantification results were exported to GraphPad Prism software for graphical illustrations.

Statistical Analysis. Statistical analyses were performed with Microsoft Excel for Mac 2011 and GraphPad Prism software. Experimental groups were analyzed by unpaired two-tailed Student's *t* test or one-way and two-way ANOVA with Tukey's multiple comparisons test. Statistical significance was considered when the *P* value was <0.05. Red circles in bar graphs show the average values of independent experiments or values for individual animals.

Data, Materials, and Software Availability. The data underlying Figs. 1, 2, and 4–7 are openly available in the publicly accessible database UCLA Dataverse at https://doi.org/10.25346/S6/Z7JORC (49). All other data are included in the manuscript and/or supporting information.

ACKNOWLEDGMENTS. We thank Stella Choi for assistance with the measurement of nuclear lamin meshwork gap sizes. This work was supported by the National Center for Advancing Translational Sciences University of California, Los Angeles Clinical and Translational Science Institute (UCLA CTSI) (UL1TR001881). Virus production and transduction were performed by the University of California, Los Angeles Vector Core, which is supported by CURE/P30 DK041301. Stimulated emission depletion (STED) microscopy was performed at the Advanced Light Microscopy/Spectroscopy Laboratory and Leica Microsystems Center of Excellence at the California NanoSystems Institute at UCLA (RRID:SCR_022789) with funding support from NIH Shared Instrumentation Grant S10OD025017 and NSF Major Research Instrumentation grant CHE-0722519.

Author affiliations: [a]Department of Medicine, David Geffen School of Medicine, University of California, Los Angeles, CA 90095; [b]Department of Bioengineering, University of California, Los Angeles, CA 90095; [c]Advanced Light Microscopy and Spectroscopy Laboratory, California NanoSystems Institute, University of California, Los Angeles, CA 90095; and [d]Department of Human Genetics, David Geffen School of Medicine, University of California, Los Angeles, CA 90095

1. M. Eriksson *et al.*, Recurrent de novo point mutations in lamin A cause Hutchinson-Gilford progeria syndrome. *Nature* **423**, 293–298 (2003).
2. M. A. Merideth *et al.*, Phenotype and course of Hutchinson-Gilford progeria syndrome. *N. Engl. J. Med.* **358**, 592–604 (2008).
3. S. G. Young, L. G. Fong, S. Michaelis, Prelamin A, Zmpste24, misshapen cell nuclei, and progeria–New evidence suggesting that protein farnesylation could be important for disease pathogenesis. *J. Lipid Res.* **46**, 2531–2558 (2005).
4. S. H. Yang *et al.*, A farnesyltransferase inhibitor improves disease phenotypes in mice with a Hutchinson-Gilford progeria syndrome mutation. *J. Clin. Invest.* **116**, 2115–2121 (2006).
5. R. Varga *et al.*, Progressive vascular smooth muscle cell defects in a mouse model of Hutchinson-Gilford progeria syndrome. *Proc. Natl. Acad. Sci. U.S.A.* **103**, 3250–3255 (2006).
6. A. Sánchez-López *et al.*, Cardiovascular progerin suppression and lamin A restoration rescue Hutchinson-Gilford progeria syndrome. *Circulation* **144**, 1777–1794 (2021).
7. M. W. Glynn, T. W. Glover, Incomplete processing of mutant lamin A in Hutchinson-Gilford progeria leads to nuclear abnormalities, which are reversed by farnesyltransferase inhibition. *Hum. Mol. Genet.* **14**, 2959–2969 (2005).
8. Y. Turgay, O. Medalia, The structure of lamin filaments in somatic cells as revealed by cryo-electron tomography. *Nucleus* **8**, 475–481 (2017).
9. T. A. Dittmer, T. Misteli, The lamin protein family. *Genome Biol.* **12**, 222 (2011).
10. Y. Turgay *et al.*, The molecular architecture of lamins in somatic cells. *Nature* **543**, 261–264 (2017).
11. T. Shimi *et al.*, Structural organization of nuclear lamins A, C, B1, and B2 revealed by superresolution microscopy. *Mol. Biol. Cell* **26**, 4075–4086 (2015).
12. B. Nmezi *et al.*, Concentric organization of A- and B-type lamins predicts their distinct roles in the spatial organization and stability of the nuclear lamina. *Proc. Natl. Acad. Sci. U.S.A.* **116**, 4307–4315 (2019).
13. N. Y. Chen *et al.*, Increased expression of LAP2β eliminates nuclear membrane ruptures in nuclear lamin-deficient neurons and fibroblasts. *Proc. Natl. Acad. Sci. U.S.A.* **118**, e2107770118 (2021).
14. H. J. Worman, E. C. Schirmer, Nuclear membrane diversity: Underlying tissue-specific pathologies in disease? *Curr. Opin. Cell Biol.* **34**, 101–112 (2015).
15. M. P. Mallampalli, G. Huyer, P. Bendale, M. H. Gelb, S. Michaelis, Inhibiting farnesylation reverses the nuclear morphology defect in a HeLa cell model for Hutchinson-Gilford progeria syndrome. *Proc. Natl. Acad. Sci. U.S.A.* **102**, 14416–14421 (2005).
16. V. L. Verstraeten, J. Y. Ji, K. S. Cummings, R. T. Lee, J. Lammerding, Increased mechanosensitivity and nuclear stiffness in Hutchinson-Gilford progeria cells: Effects of farnesyltransferase inhibitors. *Aging Cell* **7**, 383–393 (2008).

17. J. B. Kelley *et al.*, The defective nuclear lamina in Hutchinson-gilford progeria syndrome disrupts the nucleocytoplasmic Ran gradient and inhibits nuclear localization of Ubc9. *Mol. Cell Biol.* **31**, 3378–3395 (2011).
18. W. Chang *et al.*, Imbalanced nucleocytoskeletal connections create common polarity defects in progeria and physiological aging. *Proc. Natl. Acad. Sci. U.S.A.* **116**, 3578–3583 (2019).
19. W. H. De Vos *et al.*, Repetitive disruptions of the nuclear envelope invoke temporary loss of cellular compartmentalization in laminopathies. *Hum. Mol. Genet.* **20**, 4175–4186 (2011).
20. J. Zhang *et al.*, A human iPSC model of Hutchinson Gilford Progeria reveals vascular smooth muscle and mesenchymal stem cell defects. *Cell Stem Cell* **8**, 31–45 (2011).
21. P. H. Kim *et al.*, Nuclear membrane ruptures underlie the vascular pathology in a mouse model of Hutchinson-Gilford progeria syndrome. *JCI Insight* **6**, e151515 (2021).
22. N. Coll-Bonfill *et al.*, Progerin induces a phenotypic switch in vascular smooth muscle cells and triggers replication stress and an aging-associated secretory signature. *Geroscience* **45**, 965–982 (2023).
23. H. Zhang, Z. M. Xiong, K. Cao, Mechanisms controlling the smooth muscle cell death in progeria via down-regulation of poly(ADP-ribose) polymerase 1. *Proc. Natl. Acad. Sci. U.S.A.* **111**, E2261–E2270 (2014).
24. M. R. Hamczyk *et al.*, Progerin accelerates atherosclerosis by inducing endoplasmic reticulum stress in vascular smooth muscle cells. *EMBO Mol. Med.* **11**, e9736 (2019).
25. P. H. Kim *et al.*, Disrupting the LINC complex in smooth muscle cells reduces aortic disease in a mouse model of Hutchinson–Gilford progeria syndrome. *Sci. Transl. Med.* **10**, eaat7163 (2018).
26. W. Stehbens, B. Delahunt, T. Shozawa, E. Gilbert-Barness, Smooth muscle cell depletion and collagen types in progeric arteries. *Cardiovasc. Pathol.* **10**, 133–136 (2001).
27. J. D. Vargas, E. M. Hatch, D. J. Anderson, M. W. Hetzer, Transient nuclear envelope rupturing during interphase in human cancer cells. *Nucleus* **3**, 88–100 (2012).
28. C. M. Denais *et al.*, Nuclear envelope rupture and repair during cancer cell migration. *Science* **352**, 353–358 (2016).
29. F. Civril *et al.*, Structural mechanism of cytosolic DNA sensing by cGAS. *Nature* **498**, 332–337 (2013).
30. E. M. Hatch, M. W. Hetzer, Nuclear envelope rupture is induced by actin-based nucleus confinement. *J. Cell Biol.* **215**, 27–36 (2016).
31. Y. Gruenbaum, R. Foisner, Lamins: Nuclear intermediate filament proteins with fundamental functions in nuclear mechanics and genome regulation. *Annu. Rev. Biochem.* **84**, 131–164 (2015).
32. G. Bonne *et al.*, Mutations in the gene encoding lamin A/C cause autosomal dominant Emery-Dreifuss muscular dystrophy. *Nat. Genet.* **21**, 285–288 (1999).
33. C. M. Wolf *et al.*, Lamin A/C haploinsufficiency causes dilated cardiomyopathy and apoptosis-triggered cardiac conduction system disease. *J. Mol. Cell Cardiol.* **44**, 293–303 (2008).
34. E. Delbarre *et al.*, The truncated prelamin A in Hutchinson-Gilford progeria syndrome alters segregation of A-type and B-type lamin homopolymers. *Hum. Mol. Genet.* **15**, 1113–1122 (2006).
35. D. Holtz, R. A. Tanaka, J. Hartwig, F. McKeon, The CaaX motif of lamin A functions in conjunction with the nuclear localization signal to target assembly to the nuclear envelope. *Cell* **59**, 969–977 (1989).
36. E. A. Nigg, G. T. Kitten, K. Vorburger, Targeting lamin proteins to the nuclear envelope: The role of CaaX box modifications. *Biochem. Soc. Trans.* **20**, 500–504 (1992).
37. A. Buxboim *et al.*, Scaffold, mechanics and functions of nuclear lamins. *FEBS Lett.* **597**, 2791–2805 (2023).
38. S. H. Yang *et al.*, Absence of progeria-like disease phenotypes in knock-in mice expressing a non-farnesylated version of progerin. *Hum. Mol. Genet.* **20**, 436–444 (2011).
39. J. I. Toth *et al.*, Blocking protein farnesyltransferase improves nuclear shape in fibroblasts from humans with progeroid syndromes. *Proc. Natl. Acad. Sci. U.S.A.* **102**, 12873–12878 (2005).
40. S. H. Yang *et al.*, Blocking protein farnesyltransferase improves nuclear blebbing in mouse fibroblasts with a targeted Hutchinson-Gilford progeria syndrome mutation. *Proc. Natl. Acad. Sci. U.S.A.* **102**, 10291–10296 (2005).
41. Y. Wang *et al.*, Blocking farnesylation of the prelamin A variant in Hutchinson-Gilford progeria syndrome alters the distribution of A-type lamins. *Nucleus* **3**, 452–462 (2012).
42. L. B. Gordon *et al.*, Impact of farnesylation inhibitors on survival in Hutchinson-Gilford progeria syndrome. *Circulation* **130**, 27–34 (2014).
43. B. C. Capell *et al.*, A farnesyltransferase inhibitor prevents both the onset and late progression of cardiovascular disease in a progeria mouse model. *Proc. Natl. Acad. Sci. U.S.A.* **105**, 15902–15907 (2008).
44. L. G. Fong *et al.*, A protein farnesyltransferase inhibitor ameliorates disease in a mouse model of progeria. *Science* **311**, 1621–1623 (2006).
45. A. D. Basso, P. Kirschmeier, W. R. Bishop, Thematic review series: Lipid posttranslational modifications. Farnesyl transferase inhibitors. *J. Lipid Res.* **47**, 15–31 (2009).
46. T. Shimi *et al.*, The A- and B-type nuclear lamin networks: Microdomains involved in chromatin organization and transcription. *Genes Dev.* **22**, 3409–3421 (2008).
47. C. Samson *et al.*, Emerin self-assembly mechanism: Role of the LEM domain. *FEBS J.* **284**, 338–352 (2017).
48. J. M. Lee *et al.*, Modulation of LMNA splicing as a strategy to treat prelamin A diseases. *J. Clin. Invest.* **126**, 1592–1602 (2016).
49. P. H. Kim *et al.*, Progerin forms an abnormal meshwork and has a dominant-negative effect on the nuclear lamina. UCLA Dataverse. https://doi.org/10.25346/S6/Z7JORC. Deposited 12 June 2024.